Materials Science & Engineering C 121 (2021) 111845

Contents lists available at ScienceDirect

Materials Science & Engineering C

journal homepage: www.elsevier.com/locate/msec

# PAMAM dendrimers functionalised with an anti-TNF α antibody and chondroitin sulphate for treatment of rheumatoid arthritis

Isabel Matos Oliveira [a,b], Cristiana Gonçalves [a,b,c], Eduarda Pinheiro Oliveira [a,b], Rosana Simón-Vázquez [d,e], Alain da Silva Morais [a,b], África González-Fernández [d,e], Rui Luis Reis [a,b,c], Joaquim Miguel Oliveira [a,b,c,*]

[a] Biodegradables and Biomimetics of University of Minho, Headquarters of the European Institute of Excellence on Tissue Engineering and Regenerative Medicine, Avepark, Parque de Ciência e Tecnologia, Zona Industrial da Gandra, 4805-017 Barco, Guimarães, Portugal
[b] ICVS/3B's - PT Government Associate Laboratory, Braga, Guimarães 4805-017, Portugal
[c] The Discoveries Centre for Regenerative and Precision Medicine, Headquarters at University of Minho, Avepark, 4805-017 Barco, Guimarães, Portugal
[d] Inmunología, Centro de Investigaciones Biomédicas (CINBIO), Centro Singular de Investigación de Galicia, Instituto de Investigación Sanitaria Galicia Sur (IIS-GS), Universidade de Vigo, Campus Universitario de Vigo, 36310 Pontevedra, Spain
[e] Hospital Álvaro Cunqueiro, Estrada Clara Campoamor, 36312 Vigo, Pontevedra, Spain

ARTICLE INFO

*Keywords:*
Rheumatoid arthritis
Inflamed joint
PAMAM dendrimer
Chondroitin sulphate
Anti-TNF α
Polyclonal antibody

ABSTRACT

Rheumatoid arthritis is a chronic autoimmune disease characterised by joint synovial inflammation, along with cartilage and bone tissue destruction. Dendrimers can offer new opportunities as drug delivery systems of molecules of interest. Herein we aimed to develop poly(amidoamine) dendrimers (PAMAM), functionalised with chondroitin sulphate (CS), lined with anti-TNF α antibodies (Abs) to provide anti-inflammatory properties. Physicochemical characterisation demonstrated that anti-TNFα Abs-CS/PAMAM dendrimer NPs were successfully produced. The *in vitro* studies revealed that CS/PAMAM dendrimer NPs did not affect the ATDC5 and THP-1 cell lines' metabolic activity and proliferation, presenting good cytocompatibility and hemocompatibility. Moreover, anti-TNFα Abs-CS/PAMAM dendrimer NPs showed suitable TNF α capture capacity, making them appealing for new immunotherapies in RA patients.

## 1. Introduction

Modern lifestyle has been accompanied by an increased incidence of age-related and autoimmune diseases. Autoimmune disorders have several aetiologies, from genetic susceptibility or immune dysregulation to environmental factors [1,2].

Rheumatoid arthritis (RA) is a systemic autoimmune disorder with undisclosed cause, characterised by polyarthritis and joint synovial inflammation, as well as cartilage and bone tissue destruction [3].

Currently, RA treatment strategies include disease-modifying anti-rheumatic drugs (DMARDs), typically supported by non-steroidal anti-inflammatory drugs (NSAIDs) and/or corticosteroids to reduce the pain and inflammation [4]. However, many side effects are associated with these treatments, limiting their therapeutic efficacy. Therefore, it is essential to develop and validate new drug delivery strategies for RA treatment that specifically target inflamed joints and attenuate the damage to healthy tissues [5].

High levels of the pro-inflammatory Tumour Necrosis Factor alfa (TNF α) are observed in the synovial fluid and the synovium of patients with RA, making this cytokine an appealing target for treatment [6]. Furthermore, this pro-inflammatory cytokine induces the production of other pro-inflammatory cytokines such as Interleukin (IL)-1, IL-6, IL-8, and Matrix metalloproteinases (MMPs) which also play a very important role in the pathology of rheumatoid arthritis [7,8]. Targeting TNF α with anti-TNF α agents, such as antibodies (Abs) and fusion proteins, has shown to induce long-term improvements in RA manifestations and signs [9]. For this reason, several smart nanocarriers for delivering drugs have been developed and tested for RA treatment [10,11].

Dendrimers offer new opportunities as drug delivery systems with improved effectiveness and specificity. These dendrimers NPs allow a time-controlled delivery, of single or multiple compounds, reducing the uptake of toxic agents and side effects of certain drugs, while improving

* Corresponding author at: Biodegradables and Biomimetics of University of Minho, Headquarters of the European Institute of Excellence on Tissue Engineering and Regenerative Medicine, Avepark, Parque de Ciência e Tecnologia, Zona Industrial da Gandra, 4805-017 Barco, Guimarães, Portugal.
*E-mail address:* miguel.oliveira@i3bs.uminho.pt (J.M. Oliveira).

https://doi.org/10.1016/j.msec.2020.111845
Received 31 May 2020; Received in revised form 18 December 2020; Accepted 28 December 2020
Available online 6 January 2021
0928-4931/

and prolonging its bioavailability [12,13]. In particular poly(amidoamine) (PAMAM) dendrimers, polymeric structures sphere-shaped with branches, have been studied as nanocarriers for targeted drug delivery. The functional groups on the surface allow their modification to conjugate small molecules and Abs [14]. The potential of PAMAM dendrimers in the treatment of RA has been increasingly explored, and literature demonstrated that these nanoparticles allow a controlled release of molecules of interest and have anti-inflammatory properties [15,16]. Moreover, the combination of dendrimers with synthetic and natural biodegradable polymers could benefit a closer interaction with living cells, enhancing its biological performance [17]. Chondroitin sulphate (CS) is one of the main components of the extracellular matrix (ECM) and is abundant in several living tissues, such as cartilage. This sulphated glycosaminoglycan shows numerous appealing characteristics like antioxidant, antiatherosclerotic, antithrombosis, anticoagulant and non-immunogenic properties, and as a natural polymer, it is also biocompatible and biodegradable [18–20]. Moreover, considering this delivery system is intended to be administrated in the intra-articular space, and CS is one of the main components of the cartilage tissue, the functionalisation of the PAMAM dendrimers with this natural polymer may increase its affinity with the tissue of interest (cartilage).

Herein it was hypothesised that PAMAM dendrimers functionalised with CS and linked to specific Abs could have advantageous properties for the treatment of RA. Thus, this work consists of the development and evaluation of an innovative approach for RA treatment, based on targeted delivery, using an anti-TNF α Abs linked to PAMAM dendrimers. The PAMAM were functionalised with CS and synthesised as nanocarriers, to help receptor-ligand interaction and low toxicity, while the covalently linked anti-TNF α Abs provides anti-inflammatory properties.

The successful functionalisation of PAMAM dendrimer NPs was confirmed through their physicochemical characterisation, using energy-dispersive X-ray spectroscopy, proton nuclear magnetic resonance spectroscopy, Fourier transform infrared spectroscopy, Scanning Transmission Electron Microscope, Dynamic light scattering, electrophoretic light scattering, and Rheometer methodologies. *In vitro* studies were performed to analyse the effect of the PAMAM dendrimer NPs on the viability and proliferation of human chondrogenic, lymphocytic, and monocytic cells. The dendrimers' internalisation, NPs-induced haemolysis, interaction with plasma proteins, and anti-inflammatory activity were also evaluated.

## 2. Materials and methods

### 2.1. Synthesis of the CS/PAMAM dendrimer NPs

Chondroitin sulphate A sodium salt from bovine trachea (463.363 g/mol) and PAMAM carboxylic-terminated dendrimers (generation 1.5, 20% methanolic solution), with an ethylenediamine core, were purchased from Sigma-Aldrich (USA). CS/PAMAM dendrimer NPs were prepared as referred by Shaunak et al., 2004, with some modifications. Briefly, 20 g/mol of (2-N-Morpholino)ethanesulfonic acid hydrate (MES) (Sigma-Aldrich) was added to 50 g $L^{-1}$ of PAMAM (diluted in MES), then N-(3-Dimethylaminopropyl)-*N*′-ethylcarbodiimide hydrochloride (EDC) (Sigma-Aldrich, USA) (4 equivalents) and sulfo-NHS N-Hydroxysulfosuccinimide sodium salt ≥98% (HPLC) (Sigma-Aldrich, USA) (2 equivalents), also in MES, were mixed and stirred for 15 min, with the first solution of PAMAM. Then, chondroitin sulphate (20 equivalents) was added with EDC (4 equivalents) and the reactions were mixed and stirred for 15 min. The PAMAM mixture was added to the CS mixture and stirred for 24 h. The solution was dialysed against distilled water using a Dialysis Tubing membrane, benzoylated (Laborspirit, Loures), for 48 h. CS/PAMAM dendrimer NPs were obtained by freezing the solution at −80 °C and freeze-drying (Telstar-LyoAlfa 10/15) for approximately 7 days.

### 2.2. Labelling of CS/PAMAM dendrimer NPs with fluorescein isothiocyanate (FITC)

The CS/PAMAM dendrimer NPs were linked to Fluorescein isothiocyanate (FITC) (Sigma-Aldrich, USA). Firstly, 10 mg $mL^{-1}$ of CS/PAMAM solution was prepared in a carbonate-bicarbonate coupled buffer (pH 9.2). Then 50 μL of the FITC (10 mg $mL^{-1}$)/DMSO (anhydrous dimethyl sulfoxide) solution was added per each mL of CS/PAMAM dendrimer NPs solution under agitation and kept in the dark at 4 °C for 8 h. Lastly, the FITC-labelled CS/PAMAM dendrimer NPs were dialysed in ultrapure water for 48 h. The product was achieved after dialysis and freeze-drying.

### 2.3. Physiochemical characterisation

#### 2.3.1. Proton nuclear magnetic resonance spectroscopy ($^1$H NMR)

CS/PAMAM dendrimer NPs was solubilised in deuterium water oxide (1 mg $mL^{-1}$) at room temperature and the sample was transferred to NMR tube. The NMR spectra were obtained on a Bruker AVANCE 400 spectrometer, at 50 °C using a resonance frequency of 400 MHz. To process and analyse the obtained spectra, MestReNova 9.0 Software was used.

#### 2.3.2. Fourier transform infrared spectroscopy (FTIR)

The CS/PAMAM dendrimer NPs were mixed with potassium bromide and moulded into a transparent pellet using a press. Transmission spectra were acquired on an IR Prestige-21 spectrometer (Shimadzu, Japan), using wavenumber range between 4400 and 400 $cm^{-1}$, 32 scans and a resolution of 4 $cm^{-1}$.

#### 2.3.3. Energy-dispersive X-ray spectroscopy (EDS)

CS/PAMAM dendrimer NPs samples were coated with carbon (Fisons Instruments, Polaron SC 508, UK). The electric current was set at 18 mA with a coating time of 120 s. The sulphur, calcium, sodium, carbon and oxygen elemental analysis were achieved through an X-ray detector (Pentafet model 5526, UK) attached to the S-360 microscope, and a voltage of 10 kV was used.

#### 2.3.4. Dynamic light scattering (DLS) and electrophoretic light scattering (ELS)

Particle size and zeta potential of CS/PAMAM dendrimer NPs were measured in a particle analyser (Zetasizer Nano ZS, Malvern Instruments, UK). Particle size analysis was made by DLS technique, in an ultrapure water solution with 1 mg $mL^{-1}$ of CS/PAMAM dendrimer NPs. Zeta potential of nanoparticles was evaluated by ELS, at pH 7.4 phosphate buffer saline (PBS) solution.

#### 2.3.5. Atomic force microscopy (AFM)

The morphology of the nanoparticles was evaluated through AFM. The CS/PAMAM dendrimer NPs were dissolved in ultrapure water to achieve a final concentration of 1 mg $mL^{-1}$ and transferred to the surface of a 9.9 mm mica disc (Agar Scientific, England). The samples were evaluated using the Tapping model TM with a MultiMode AFM connected to a NanoScope III controller (Veeco, USA) with noncontact silicon nanoprobes (*ca.* 300 kHz) from Nanosensors, Switzerland. Images were plane-fitted using the third-degree-flatten procedure included in NanoScope software version 1.5. The particle morphology and size were both analysed with NanoScope 1.5 software.

#### 2.3.6. Scanning Transmission Electron Microscope (STEM)

The size and morphology of CS/PAMAM dendrimer NPs were also obtained by STEM. The nanoparticles were diluted in ultrapure water to a final concentration of 0.1 mg $mL^{-1}$ and then 2 μL were placed on copper grids at 37 °C overnight for observation.

#### 2.3.7. Rheometer methodologies

Rheological analyses were performed using Kinexus pro+rheometer with the acquisition software rSpace (Malvern). The rotational experiments were performed using a cone-plate measuring system composed by an upper stainless-steel cone of 40 mm of diameter and a cone angle of 4°. Shear viscosity was obtained as a function of the shear rate, from 0.001 to 0.1 $s^{-1}$ at 37 °C. The oscillatory experiments were made to obtain frequency sweep curves, after LVER determination.

## 3. TNF-α Abs linked to CS/PAMAM dendrimer nanoparticles

### 3.1. Functionalisation

The CS/PAMAM dendrimer NPs linked to rabbit polyclonal anti-TNF-α antibodies (ab7742, Abcam, United Kingdom) was obtained through a crosslinking reaction. A 0.2 g $L^{-1}$ solution of CS/PAMAM in 5 mL MES was mixed with EDC (4 equivalents) and NHS (2 equivalents) for 15 min. Next, 20 equivalents of anti-TNF α Abs were added with EDC (4 equivalents) and were stirred for 15 min. Then, CS/PAMAM dendrimer NPs mixture was added to anti-TNF α Abs mixture and stirred for 24 h. The solution was dialysed against distilled water for 48 h. Anti-TNF α Abs-CS/PAMAM dendrimer NPs were obtained through dialysis and freeze-drying.

### 3.2. Physicochemical characterisation

The immobilisation of the Abs by CS/PAMAM was evaluated by fluorescence spectrometer FP-8500 (Jasco). Briefly, anti-TNF α Abs-CS/PAMAM dendrimer NPs and CS/PAMAM dendrimer NPs were mixed with a secondary antibody anti-rabbit IgG-labelled with Alexa Fluor 488 dye (Molecular probes, USA), in PBS solution (1:1000) for 1 h to detect the conjugation of anti-TNF α Abs to CS/PAMAM dendrimer NPs. The solutions were centrifuged, and the supernatants were visualised in the spectrometer.

The determination of the degree of TNF α captured by anti-TNF α Abs-CS/PAMAM dendrimer NPs was analysed by the incubation of the dendrimers with 1000 pg $mL^{-1}$ of TNF α (Peprotech, United Kingdom) for 6 h at room temperature. After centrifugation, the supernatants were kept at −80 °C for further analysis. Then, the free TNF-α concentration in the samples after incubation was measured using a Human TNF-alpha DuoSET ELISA kit (R&D systems, USA) and a DuoSet Ancillary Reagent Kit 2 (R&D systems, USA). The calibration curve was prepared using TNF-α standard solutions, with concentrations from 0 to 1000 pg $mL^{-1}$, which were also included in the ELISA plate. The samples were measured in the microplate reader (Synergy HT, BIO-TEK) with an optical density of 450 nm.

## 4. *In vitro* studies

### 4.1. Cell cultures

Chondrogenic ATDC 5 cell line (European Collection of Authenticated Cell Culture, England), human monocytic cell line (THP-1) and differentiated human T lymphocyte cell line (Jurkat) were used to analyse the effects of CS/PAMAM dendrimer NPs in cartilage and immune system cells.

ATDC 5 cell line was expanded in DMEM medium (Dulbecco's Modified Eagle Medium: Nutrient Mixture F-12, Alfagene, Portugal). THP-1 and Jurkat cell lines were expanded in RPMI medium (RPMI 1640 Medium, GlutaMAX™ Supplement, HEPES, Gibco, Life Technologies, Grand Island, NY), supplemented with 10% Heat Inactivated Foetal Bovine Serum, 2 mM glutamine and 100 U $mL^{-1}$ of penicillin/streptomycin (PAA; Pasching, Austria), under standard culture conditions (37 °C in a humidified atmosphere, containing 5 v/v $CO_2$).

The experiments with the THP-1 and Jurkat cells were carried out in the Immunology laboratory at the University of Vigo and for that reason, some experimental conditions differ from the ATDC 5 cell line. When the conditions or the equipment used were different, it was specifically mentioned.

### 4.2. MTS assay

Cell viability was evaluated by MTS [3-(4,5-dimethylthiazol-2-yl)-5-(3-carboxymethoxyphenyl)-2(4-sulfophenyl)-2H-tetrazolium] (VWR International, USA). The ATDC 5 cells were seeded at a density of $1 \times 10^4$ cells per well and incubated with different concentrations of CS/PAMAM dendrimer NPs, for 72 h. Cells cultured with regular medium (without CS/PAMAM dendrimer NPs) were used as a control. At each time point, cell culture medium (DMEM-F12) was replaced by culture medium without phenol red, containing MTS at a 5:1 ratio, and was incubated for 3 h. Then, 100 μL from each well were passed into a 96-well plate and the absorbance was read at 490 nm.

The Jurkat and (differentiated) THP-1 cell lines were seeded in a 96-well plate with a density of $3 \times 10^4$ and $1 \times 10^4$ cells per well, respectively. The CS/PAMAM dendrimer NPs were administrated in serial dilutions 1:2 starting with the concentrations of 0.5 mg $mL^{-1}$. The cells were incubated with the CS/PAMAM dendrimer NPs for 48 h, in standard cell culture conditions. The remaining procedure was performed as previously mentioned for the ATDC 5 cell line.

### 4.3. DNA quantification

The proliferation of the ATDC5 cells upon CS/PAMAM dendrimer NPs administration was analysed by DNA quantification, using the Quanti-IT PicoGreen dsDNA Assay Kit (Alfagene, Portugal).

ATDC5 cells were seeded at a density of $1 \times 10^4$ cells per well and incubated with different concentrations of CS/PAMAM dendrimer NPs for 72 h. Cells cultured with DMEM-F12 medium were used as control. After the incubation period, the cells were lysed in ultrapure water and stored at −80 °C for further analysis. The calibration curve was performed using DNA standards, prepared with concentrations ranging from 2 to 0 μL $mL^{-1}$. Both the calibration curve and the cells' samples were quantified following the manufacturer's instructions. The fluorescence was acquired at 480/20 nm of excitation and emission of 528/20 nm, in a microplate reader. The DNA concentration on the cells samples was determined using the standard curve.

### 4.4. Flow cytometry

For flow cytometry analysis the ATDC 5 cells were seeded at a density $4 \times 10^5$ cells per well (in a 24-well plate) and cultured with different concentrations of FITC-labelled CS/PAMAM NPs (0.01, 0.1 and 0.5 mg $mL^{-1}$), for 72 h. ATDC5 cells cultured in DMEM-F12 without CS/PAMAM dendrimer NPs were used as control. The samples were measured using a FACSCalibur flow cytometer (BD Biosciences Immunocytometry Systems, CA, USA) and the results were analysed by the Flowing Software 2. THP-1 cells were incubated for 3, 6 and 24 h with 0.5 mg $mL^{-1}$ of CS/PAMAM dendrimer NPs at a cell density of $1 \times 10^5$ cells per well, in a 24-well plate. THP-1 cells cultured with only RPMI medium were used as control. The samples were measured in a BD Accuri C6 flow cytometer (BD Biosciences, USA) and the analysis was performed in the cytometer software.

### 4.5. Fluorescence microscopy

For this assay the ATDC5 cells were seeded at a density of $1 \times 10^4$ cells per well in a 24-well plate, with different concentrations of FITC-labelled CS/PAMAM dendrimer NPs, using the previously tested time points. Then, cells were fixed with 10% formalin (Sigma-Aldrich, USA) and stained with 4,6-diamidino-2-phenylindole, dilactate (DAPI blue, VWR International, USA) for nuclei and Texas Red-X phalloidin (Sigma-Aldrich, USA) for actin filaments of the cytoskeleton. The cells were

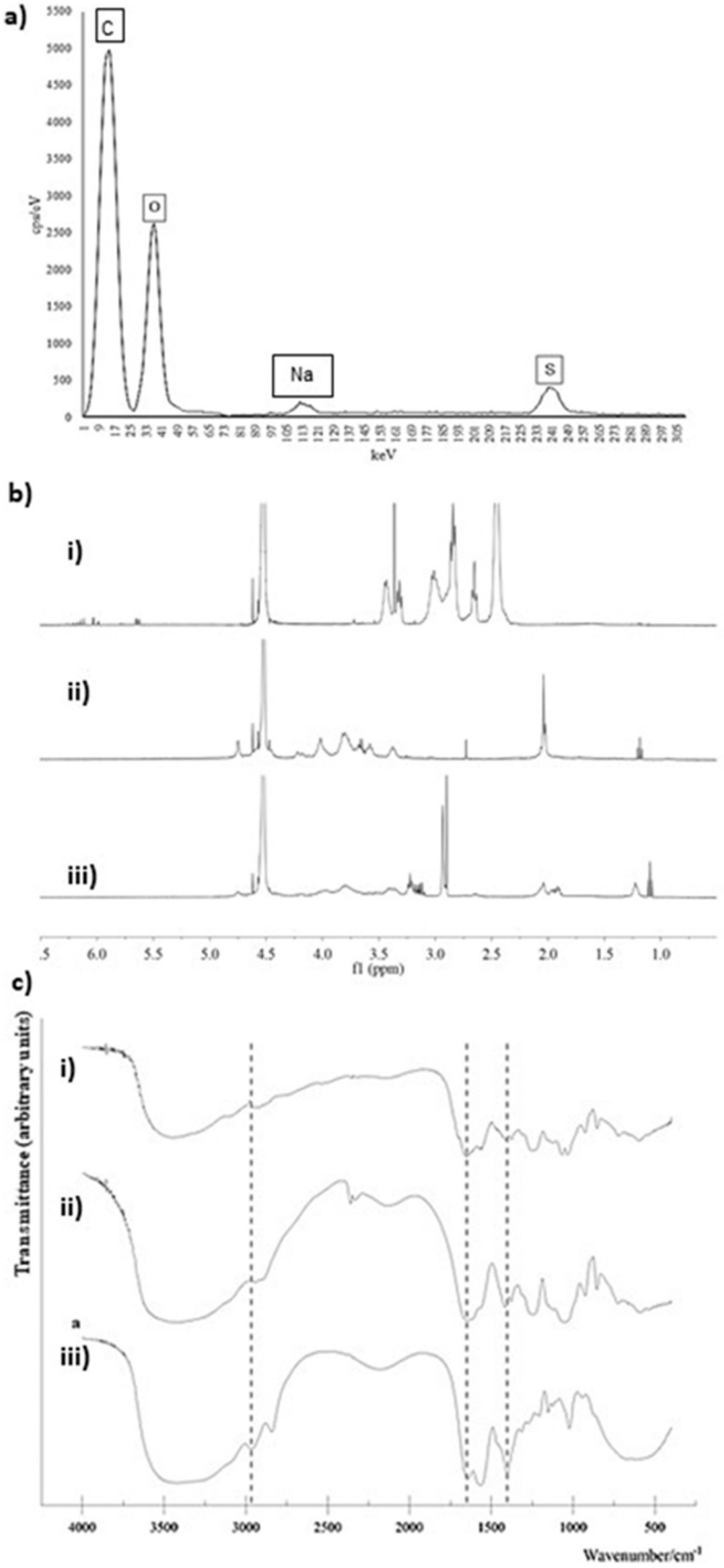


**Fig. 1.** EDS analysis (a) of CS/PAMAM dendrimer and $^{1}$H NMR in D2O at 50 °C (b) and FTIR (c), of PAMAM dendrimer (G = 1.5) (i), CS (ii) and the CS/PAMAM dendrimer NPs (iii).

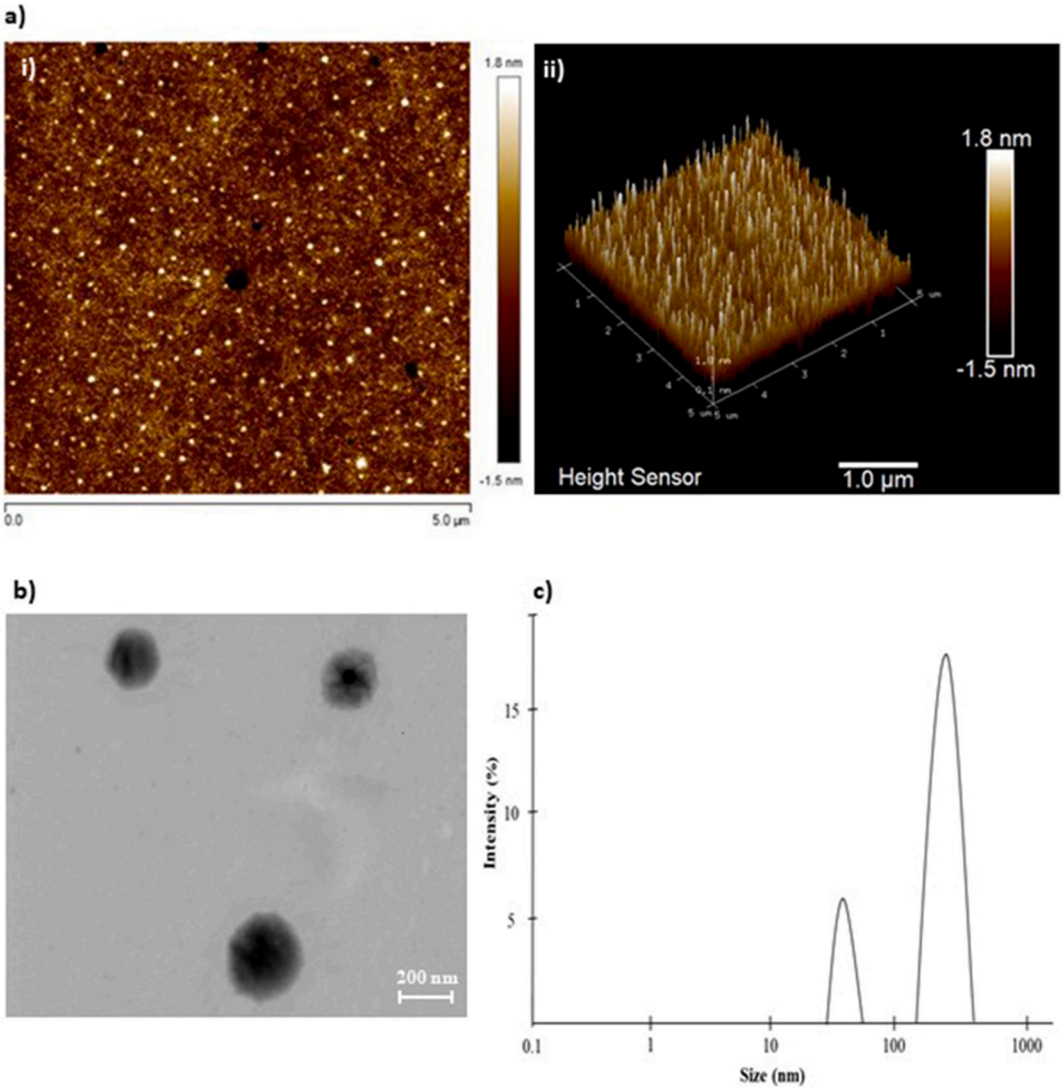


**Fig. 2.** (a) AFM analysis (i) 2D, (ii) 3D (b) STEM analysis of the CS/PAMAM dendrimer NPs and (c) DLS analysis.

observed under the fluorescence microscope (Axiolmager, Z1, Zeis Inc., Oberkochen, Germany).

The differentiated THP-1 cells were seeded at a density of $4 \times 10^4$ cells per well in a 24-well plate and incubated for 3 and 6 h with FITC-labelled CS/PAMAM dendrimer NPs. At each time point the cells were stained with Hoechst 33342 (1:1000) (Immnochemistry Technologies) and observed under a Nikon Eclipse Ti2 microscope (Nikon Instruments, Inc.).

### 4.6. Haemolytic properties of CS/PAMAM dendrimer NPs

Erythrocytes from whole mouse blood were used to test the haemolytic properties of CS/PAMAM dendrimer NPs. The blood was extracted into a tube with EDTA and an aliquot of 5 mL was diluted with PBS (1:10) in a pre-weighted tube. After centrifugation and washing steps, the pellet was weighed and diluted with PBS to a final concentration of 3% w/v.

The CS/PAMAM dendrimer NPs were diluted in PBS and administrated in serial dilutions 1:2 starting with the concentrations of 0.5 mg $mL^{-1}$. PBS and Triton x-100 were used as negative control and positive control, respectively. The plates were incubated for 4 h, centrifuged and the supernatant was collected. The samples were read at 588 nm absorbance using a microplate reader (Greiner Bio-one). The percentage of haemolysis in the samples was calculated according to the following Equation:

$$\text{Haemolysis}\ (\%) = \frac{\text{Abs (sample)} - \text{Abs (PBS)}}{Abs\ (Triton) - Abs\ (PBS)} \times 100$$

Abs: Absorbance at 558 nm

### 4.7. Assessment of binding to plasma protein by fluorescence spectroscopy

Suspensions of human albumin (HSA) and fibrinogen (Sigma-Aldrich, USA) at 400 µg $mL^{-1}$ and 40 µg $mL^{-1}$, respectively, were prepared in PBS. Different volumes of a CS/PAMAM dendrimer NPs solution at 0.5 mg $mL^{-1}$, or PBS as the control, were sequentially added to the cuvette (1, 5, 10 and 20 µL). The fluorescence spectra of the plasma proteins were recorded after each addition using the microplate reader. Fibrinogen was excited at 280 nm and HSA at 290 nm and the emission spectra were both collected from 300 nm to 450 nm. The spectra were obtained using the FluorEssenceTM software.

## 5. Assessment of TNF α capture by anti-TNF α Abs-CS/PAMAM dendrimer NPs

The therapeutic efficacy of the NPs was evaluated in a cell inflammation model, by assessing the anti-TNF α Abs-CS/PAMAM dendrimer NP's ability to capture TNF α in the medium. Macrophage-differentiated

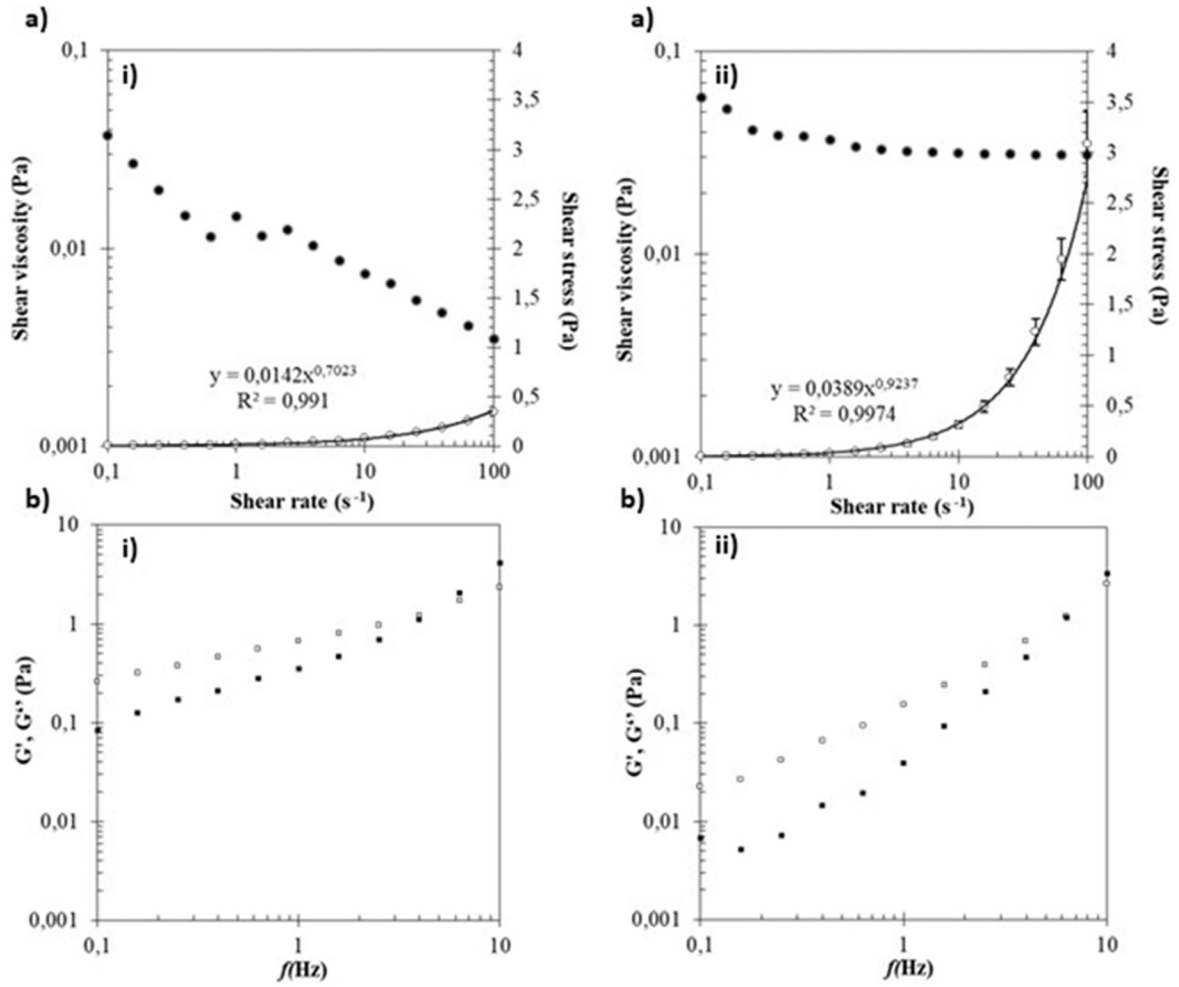


**Fig. 3.** Rheological rotational (a) and oscillatory (b) assays performed at concentrations 0.1 mg $mL^{-1}$ (i) and 0.5 mg $mL^{-1}$ (ii) of CS/PAMAM dendrimers.

THP-1 cells were stimulated with Lipopolysaccharide (LPS) (Sigma-Aldrich, USA) and used as *in vitro* model for cell inflammation. Firstly, THP1 cells were seeded at a density of $1 \times 10^6$ cells/mL in RPMI with 100 nM phorbol 12-myristate-13-acetate (PMA) (Sigma-Aldrich, USA). After 24 h of incubation time, the medium in the wells was replaced with RPMI medium without PMA and incubated for another 48 h. In order to induce an inflammatory response, 100 ng $mL^{-1}$ of LPS in RPMI medium were added to the macrophage-differentiated THP-1 cells, and the plate was incubated for 5 h. After LPS stimulation, 0.5 mg $mL^{-1}$ of anti-TNF α Abs-CS/PAMAM dendrimer NPs were added to the cells, using a medium with only PMA were used as control. At each time point (1 day, 3 days, and 7 days), the culture medium was removed from the wells, centrifugated and the supernatants were stored at −80 °C for further analysis.

To determine the degree of TNF α captured by the anti-TNF α Abs-CS/PAMAM dendrimer NPs, the TNF-α concentration in the samples was measured using the Human TNF-alpha DuoSET ELISA kit (R&D systems, USA) and the DuoSet Ancillary Reagent Kit 2 (R&D systems, USA). The calibration curve was performed using TNF-α standard solutions, with concentrations ranging from 1000 to 0 pg $mL^{-1}$, which were also included in the ELISA plate. The samples were analysed using a microplate reader, with an optical density of 450 nm (Synergy HT, BIO-TEK).

## 6. Statistical analysis

Statistical analysis was performed using GraphPad Prism 8 version. Statistical significances were determined as *$p < 0.05$, ** $p < 0.01$ and *** $p < 0.001$. All assays were performed in triplicated and results were presented as mean ± standard deviation.

## 7. Results and discussion

### 7.1. Physicochemical characterisation

#### 7.1.1. Chemical analysis of CS/PAMAM dendrimer NPs

This study focused on the functionalisation of PAMAM with CS, conjugated to an anti-TNF α Abs. It was hypothesised that this strategy can be used for RA treatment, by helping receptor-ligand interaction, reducing toxicity, and providing anti-inflammatory properties. The first steps consisted of the functionalisation of PAMAM dendrimer NPs with CS and, later on, with anti-TNF α Abs. Then, it was followed by the physicochemical characterisation and further evaluation of their biological effect.

Firstly, the successful functionalisation of the PAMAM with CS was confirmed through chemical analysis. Fig. 1 shows EDS analysis, $^1H$ NMR and FTIR spectra of the CS/PAMAM dendrimer NPs.

The EDS analysis showed the presence of C, O, and Na atoms at a percentage of 58.3%, 34.5% and 0.3%, respectively (Fig. 1a). The analysis of functionalised PAMAM also detected a sulphur group (6.9%) that does not exist on the PAMAM structure but is a characteristic chemical element of chondroitin sulphate, suggesting the PAMAM dendrimer's modification with CS was accomplished [21,22].

The PAMAM dendrimer is a branched polymer with an abundance of

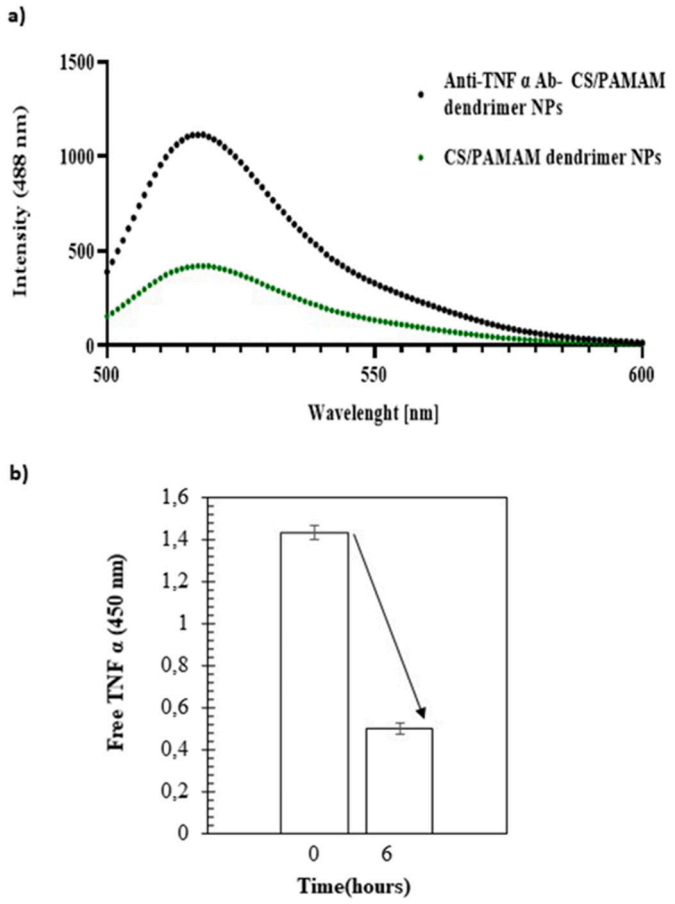


**Fig. 4.** a) Fluorescence spectroscopy of CS/PAMAM dendrimer NPs and anti-TNF α Abs-CS/PAMAM dendrimer NPs. b) Percentage of TNF α captured by anti-TNF α Abs-CS/PAMAM dendrimer NPs.

protons, making the identification of full structure on the $^{1}$H NMR and FTIR spectrum a challenge. Nevertheless, some characteristic chemical shifts can be identified, such as the well-defined signals visible on the $^{1}$H NMR spectra (Fig. 1b). Typical shifts of PAMAM dendrimer were observed at 2.4, 2.6, 2.7, 2.8 and 3.5 ppm [23,24] but also chemical shifts of chondroitin sulphate (CS-A sodium salt from bovine trachea) were found. The signal at 2.04 ppm corresponds to the $CH_3$ and at 4.75 ppm to the $^{1}$H signal of the 4-sulfated site of the galactosamine unit of chondroitin sulphate, following the literature [25,26]. Therefore, in the functionalised NPs it was observed the presence of characteristics peaks from both the PAMAM and CS, indicating the modification was successful. Some EDC residues were also observed specifically the chemical shifts of 1.1 ppm and 1.9 ppm. The modification was further confirmed by the FTIR analysis of the chondroitin sulphate, PAMAM dendrimer, and CS/PAMAM dendrimer NPs (Fig. 1c). In the spectra of CS/PAMAM dendrimer NPs it was visible the strong and broad peak of absorption at around 3400 $cm^{-1}$, assigned to the stretching vibration of the structural N—H overlapping the O—H stretching [27]. Other characteristic absorption bands are noticeable, for instance: 1650 $cm^{-1}$ for amide bands, 1240 $cm^{-1}$ for S═O stretching vibration, 1415 $cm^{-1}$ and 1379 cm-1 for the coupling of the C—O stretching vibration and O—H variable-angle vibration of –COOH, as described in the literature [28]. The absorption band assigned to the α-(1,4) glycoside bond was observed at 925 $cm^{-1}$ [27]. Regarding the PAMAM G1.5 spectra, it was also detectable the leading characteristic bands such as a characteristic –C = O stretching vibrations around 1645 $cm^{-1}$ due to the presence of a free ester (C = O) group. At the end, expected on half the generation material [29], and a peak at 1560 $cm^{-1}$ assigned to an O—H or N—H stretching vibration. Moreover, peaks at 2970 $cm^{-1}$ and 2840 $cm^{-1}$ assigned to –CH3 and –CH2– stretching vibrations as well as the broad peak around 3430 $cm^{-1}$ attributed to an O—H stretching vibration were also observed [27,30]. The CS/PAMAM dendrimer NPs spectrum showed a very similar spectrum to the CS, which is expected from a successful modification, due to the surface coverage allowed by such a large molecule. However, CS is a large molecule able to cover the PAMAM surface, being possible that it hides some of the PAMAM characteristic peaks.

### 7.1.2. Morphology, size and zeta potential of CS/PAMAM NPs

The morphology of the CS/PAMAM dendrimer NPs was evaluated in dry conditions, using AFM and STEM techniques, and in wet conditions by DLS and ELS, Fig. 2.

The characterisation clearly showed that CS/PAMAM dendrimer NPs had a globular shape, were monodisperse and presented a polymer coating around PAMAM dendrimer NPs, which is in accordance with the data found in literature, with/using modified PAMAM dendrimer NPs [24,31].

DLS and ELS were also used to analyse the CS/PAMAM dendrimer NPs. The data obtained by DLS (Fig. 2c) showed the presence of two peaks, one small peak with an intensity of approximately 48 nm corresponding to the modified dendrimer (i) and a second peak with an intensity of approximately 300 nm that corresponds to aggregated NPs (ii). The aggregation NPs can be caused by the interactions between non-covalent free sulphur groups/carboxyl groups of Chondroitin sulphate and/or not functionalised PAMAM dendrimer NPs (carboxyl-terminal dendrimer) and amino groups of Chondroitin sulphate [32]. Moreover, zeta potential data indicated that CS/PAMAM dendrimer NPs in PBS, at neutral pH, presented negative charge of approximately −15 mV. The data showed that the negatively charged sulphur groups in CS/PAMAM dendrimer NPS were mostly distributed at the surface of the nanoparticles, as observed in other studies [33], which once again reveals the effectiveness of the functionalisation of PAMAM dendrimer NPs with CS.

### 7.1.3. Rheological properties of CS/PAMAM dendrimer NPs

Drug delivery requires minimally invasive deployment strategies, therefore, the biomaterial used needs to have a suitable flow rate (even at the maximum pressure applicable), and be easily injected without being affected or deformed [34]. The rheological examination was performed using the rotational and oscillatory modes, resulting in flow behaviour and mechanical analysis of the produced NPs. Flow behaviour is described by the fitting of the experimental data with the power-law model: $\tau = k \cdot \gamma^{n}$, where $\tau$ is the shear stress (Pa), $\gamma$ is the shear rate ($s^{-1}$), $k$ is the consistency coefficient (Pa.sn) and $n$ is the flow behaviour index, being $n = 1$ for Newtonian liquid, $n < 1$ for shear-thinning fluid (non-Newtonian) and $n > 1$ for swelling plastic fluid [35]. Fig. 3 shows the rheological analysis of the CS/PAMAM at 0.1 mg $mL^{-1}$ and 0.5 mg $mL^{-1}$, from rotational and oscillatory experiments.

The shear-thinning behaviour of both solutions was clearly shown by the plot of the viscosity in the function of shear rate curves. Moreover, from the flow curves it was obtained the flow behaviour index for each solution, which is approximately 0.70 and 0.92 for 0.1 mg $mL^{-1}$ and 0.5 mg $mL^{-1}$ CS/PAMAM solutions, respectively. These values categorise the samples as shear-thinning fluid, having the highest concentration a more stable behaviour when higher stress was applied. Usually, shear-thinning fluids are characterised by high viscosity in static conditions and in dynamic conditions with a viscosity close to water (n = 1), thus decreasing the pressure during injection and facilitating their administration [36]. The obtained results are in accordance with the previous experiments because CS/PAMAM dendrimer NPs have a viscosity close to the water, mainly at the highest concentration (0.5 mg $mL^{-1}$). Thus, nanoparticles have a good flow behaviour to be injected.

### 7.1.4. Anti-TNF-α binding determination

The CS/PAMAM dendrimer NPs were conjugated to a polyclonal

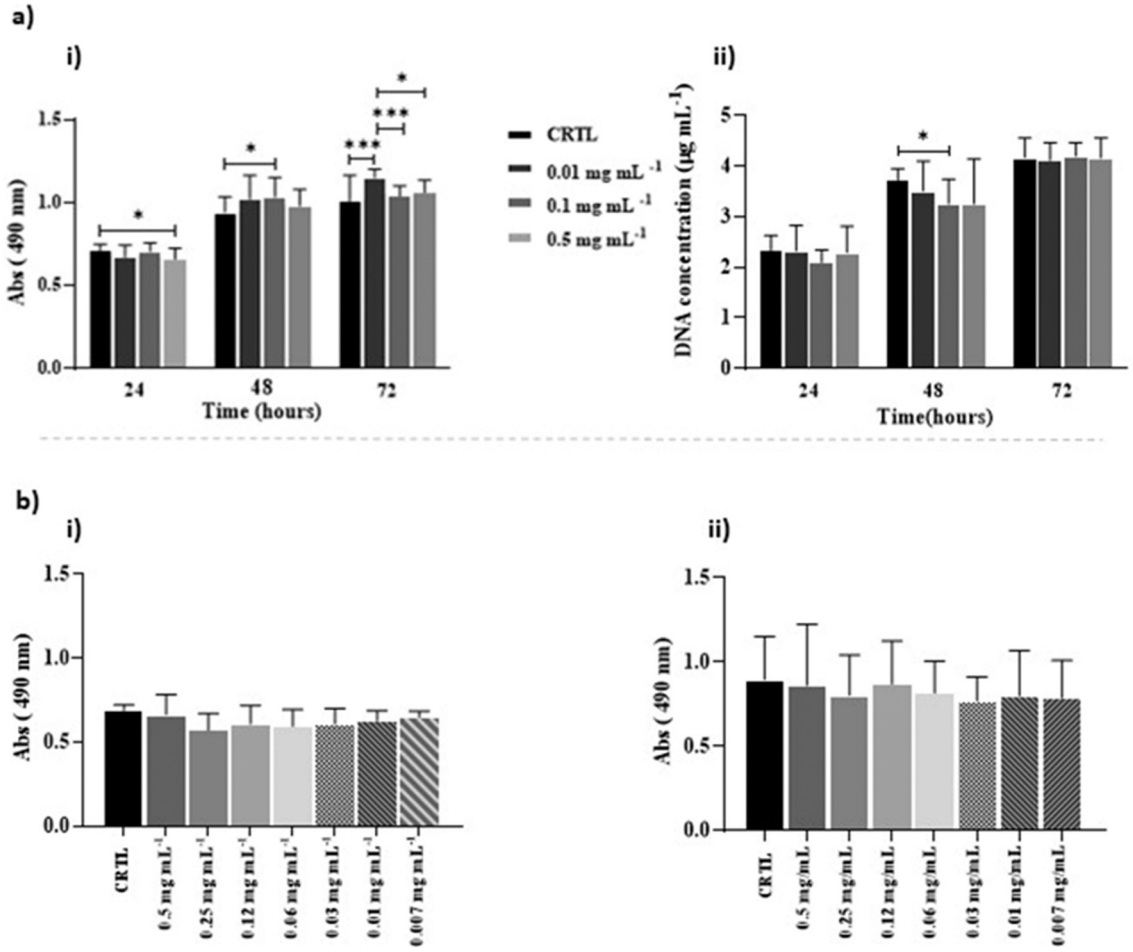


**Fig. 5.** MTS assay (a, i) and DNA quantification (a, ii) of the ATDC 5 cells. THP1 cells (b, i) and Jurkat cells' (b, ii) MTS assay. In image a) the cells were incubated with media (CTRL) and different CS/PAMAM dendrimer NPs concentrations C1, C2 and C3 (0.01, 0.1 and 0.5 mg $mL^{-1}$) at different time points (24, 48 and 72 h). In b) the cells were incubated with the CS/PAMAM dendrimer NPs at 0.5 mg $mL^{-1}$ for 48 h. Significant differences * $p < 0.001$ and *$p < 0.05$, by non-parametric Kruskal-Wallis test (a,i), (a,ii) and (b,ii); Ordinary one-way ANOVA (b,i). THP1 and Jurkat cells have not significant differences.

rabbit anti-TNF-α Abs, and to evaluate their effectiveness, fluorescence spectroscopy was performed using CS/PAMAM dendrimer NPs with and without linked Abs, in the presence of secondary antibodies labelled with Alexa Fluor 488 dye, Fig. 4.

The emission spectra of Alexa 488 (between 500 and 600 nm) for the CS/PAMAM dendrimer NPs without anti-TNF α Abs showed a low fluorescence intensity (≃400), indicative of some unspecific secondary Abs binding. However, the fluorescence of the anti-TNF α Ab-CS/PAMAM dendrimer NPs was significantly higher (≃1100), thus suggesting the conjugation with the anti-TNF α Abs was accomplished.

The anti-TNF α Abs-CS/PAMAM dendrimer NP's capacity to capture TNF α was evaluated by the difference between the initial and the final amount of free TNF α in solution, after adding the dendrimer NPs. The results demonstrated that after 6 h of reaction, between TNF α and anti-TNF α Abs-CS/PAMAM dendrimer NPs, the degree of capture was 65.27%, Fig. 4b. By maintaining this capture rate, the maximum can be reached in less than 24 h. The size of the CS/PAMAM dendrimers NPs after antibody binding was 58 ± 2.3 nm and the zeta potential −8.3 mV ± 5.7, indicating the NPs increased in size and became less negative after binding with antibody. Literature reports that positively charged particles are typically internalised by cells more extensively than negatively charged nanoparticles [37,38]. On the other hand, positive nanoparticles are more toxic [39]. For that reason, the negatively charged surface of the NPs would favour the cytocompatibility, and in turn, the NPs could be specifically internalised or bound to TNF α expressing cells, avoiding unspecific cell entry.

### 7.2. *In vitro studies*

The cell viability and proliferation upon CS/PAMAM dendrimer NPs administration and their internalisation, haemolytic properties, interference with plasma proteins, and therapeutic efficacy was assessed using the chondrogenic ATDC 5 cell line, PMA macrophage-differentiated THP-1 and T lymphocytic (Jurkat) cell lines, as models of target cells.

#### 7.2.1. *Influence of CS/PAMAM dendrimer NPs of ATDC 5, THP1 and Jurkat on cell viability and proliferation*

The influence of CS/PAMAM dendrimer NPs on cell viability and proliferation was evaluated by MTS and DNA quantification assays (Fig. 5(a) (i) and (ii), respectively), using three different concentrations of NPs (0.01, 0.1 and 0.5 mg $mL^{-1}$) on the ATDC5 cell line for 3 days.

The MTS and DNA quantification results demonstrated that although there were some significant differences between the tested NPs concentrations, the cell viability and proliferation increased over time in a similar trend than control cells. The cytotoxicity of PAMAM dendrimer depends actively on their generation and nature of functional surface groups, where high generations and cationic terminal groups often exhibit high toxicity, whereas anionic and neutral dendrimers show small or no toxic effects. Furthermore, modification of the dendrimer's surface with negatively charged or neutral moieties decreases its cytotoxicity [40]. The obtained results are in the accordance with data reported in the literature, as the produced negatively charged CS/PAMAM

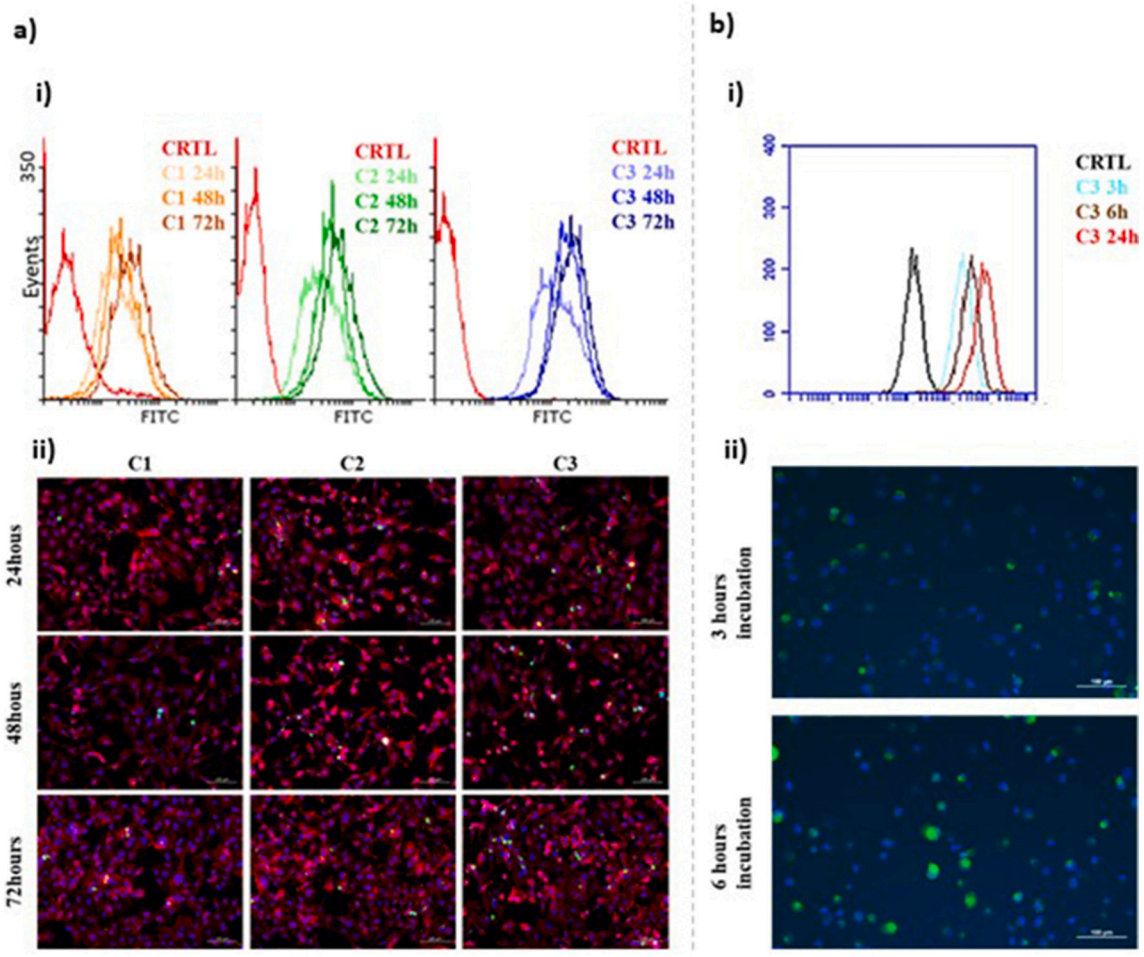


**Fig. 6.** Flow cytometry histograms (a) (i) and Fluorescence microscopy images (a) (ii) of the ATDC 5 cell line cultured in presence of different concentrations (C1 (0.01 mg $mL^{-1}$), C2 (0.1 mg $mL^{-1}$) and C3 (0.5 mg $mL^{-1}$)) of FITC labelled CS/PAMAM dendrimer NPs for 72 h. Flow cytometry (b) (i) and Fluorescence microscopy (b) (ii) of differentiated THP-1 cells with CS/PAMAM dendrimer NPs incubation at different time points (3 and 6 h). Cell nuclei are stained in blue (Hoechst) and CS/PAMAM dendrimer NPs in green (FITC). Scale bar: 100 μm (b). (For interpretation of the references to colour in this figure legend, the reader is referred to the web version of this article.)

**Table 1**
Percentage of internalisation of FITC labelled CS/PAMAM dendrimer NPs by ATDC5 cells at different concentrations of dendrimer and time points.

| Internalisation (%) | | | |
|---|---|---|---|
| Conditions/time (H) | 24 h | 48 h | 72 h |
| C1: 0.01 mg/mL | 45.98% | 56.08% | 74.19% |
| C2: 0.1 mg/mL | 66.90% | 91% | 95.32% |
| C3: 0.5 mg/mL | 98.99% | 99.36% | 99.88% |

dendrimer NPs demonstrated no harmful effects on both cell viability and proliferation in the ATDC 5 cell line.

Besides evaluating the metabolic activity and cell proliferation of NPs in ATDC 5 cells, it is vital to study their effect on the immune system. When immune cells are exposed to the stimulation they can activate several signalling pathways that promote different responses, such as proliferation, differentiation, migration, and inflammatory and immune response [41]. Macrophages are relevant cells of the innate immune system, implicated in the recognition of foreign pathogens, such as nanoparticles, *via* interaction of their surface structures with different types of Pattern Recognition Receptors (PRRs). These cells are also responsible for the production of pro-inflammatory and anti-inflammatory cytokines and pathogen clearance by phagocytosis [42]. In fact, TNF-α is released by immune cells such as macrophages or lymphocytes [43]. Having this in mind, the effect of CS/PAMAM dendrimer NPs on THP-1 and Jurkat cell line was assessed (Fig. 5b). The results obtained in the MTS assay indicated that CS/PAMAM dendrimer NPs were cytocompatible at all the tested concentrations, in both cell lines. Moreover, there were no significant differences in the cells' metabolic activity after dendrimer administration, when compared with the control cells.

### *7.2.2. Internalisation of the CS/PAMAM NPs by ATDC 5 and THP-1 cell lines*

The quantitative and qualitative analysis of the internalisation of FITC-labelled dendrimer NPs by cells was performed by flow cytometry assay and fluorescence microscopy, using ATDC 5 and THP-1 cell lines, Fig. 6.

ATDC 5 cells were cultured with different concentrations of fluorescently labelled dendrimer NPs and flow cytometry analysis showed that all concentrations obtained a high percentage of internalisation at 72 h (Fig. 6(a) (i)). NPs at 0.5 mg $mL^{-1}$ reached the highest and constant rate of internalisation over time (Table 1).

Qualitative images obtained with a fluorescence microscope showed typical morphology of the cells (marked by DAPI and phalloidin), suggesting survival and healthy proliferation in all the tested concentrations (Fig. 6(a) (ii)). The results showed that C3 (0.5 mg $mL^{-1}$) obtained almost the maximum internalisation rate at 24 h. For that reason, henceforth the experiments were performed with only the concentration

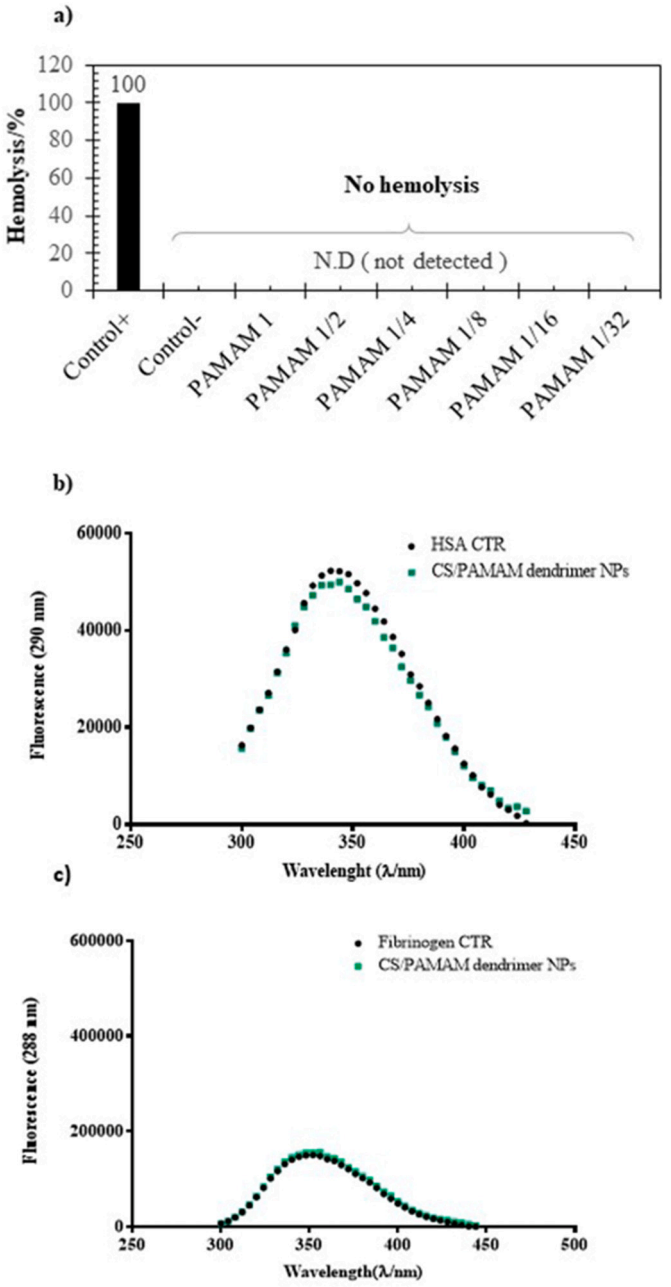


**Fig. 7.** Percentage of Haemolysis induced by the CS/PAMAM dendrimer NPs at different dilutions in contact with blood cells (a) and tryptophan emission spectra of an HSA (b) and fibrinogen (c) protein suspension in PBS, before and after incubation with CS/PAMAM dendrimer NPs at 20 μg $mL^{-1}$.

of 0.5 mg $mL^{-1}$ of CS/PAMAM dendrimer NPs.

The macrophage-differentiated THP-1 cell line was also analysed as they are phagocytic cells and can internalise dendrimers on a large scale. The FITC-labelled CS/PAMAM dendrimer NPs at 0.5 mg $mL^{-1}$ were incubated with THP-1 cells at different time points. The flow cytometry analysis showed that the internalisation rate was high after 3 h of incubation, in comparison with the control, and increased throughout the incubation time (Fig. 6(b) (i)). The internalisation of the CS/PAMAM dendrimer NPs by the macrophage cells was further confirmed by fluorescence microscopy, as depicted in Fig. 6(b) (ii).

Fluorescence microscopy confirmed the internalisation of the CS/PAMAM dendrimer NPs, detected also by flow cytometry. The microscopy images showed that after 3 h and 6 h of incubation the cells internalised the dendrimers in a high rate and that the CS/PAMAM dendrimer NPs were present in both the nucleus and cytoplasm of the cells. Despite the high internalisation rate of the dendrimers in ATDC 5 and macrophage-differentiated THP-1 cells, there was not a reduction on the cell viability, as seen in Fig. 5. Hence, the use of the CS/PAMAM dendrimer NPs for the targeted delivery of anti-TNF α Abs antibody could be a promising strategy to reduce the inflammation, based on the high internalisation rate and the absence of negative effects on the macrophage viability. Moreover, CS/PAMAM dendrimer NPs could be used to explore other therapies targeting inflammatory macrophages.

### *7.3. Haemolytic properties and interaction of the CS/PAMAM dendrimer NPs with plasma proteins*

Nanoparticles for medical applications must be subjected to biocompatibility assessments before their approval for administration in patients. The *in vitro* evaluation of the hemocompatibility is an essential part of preclinical development for NPs that will be injected through the intravenous route, or any other route in which they can be in contact with blood [44]. According to the American Society for Testing and Materials (ASTM), medical devices that have direct or indirect blood contact must not be haemolytic [45]. Following the ASTM guidelines, a biomaterial that induces the lysis of about 0% to 2% of the red blood cells is not considered haemolytic. When the burst of blood cells is about 2% to 5%, the material is partially haemolytic. For values superior to 5%, it indicates an apparent haemolytic effect [46].

The physicochemical properties of nanoparticles can also drastically influence plasm protein's functions and might originate adverse effects, such as conformational changes, which can affect their stability and loss of protein functionality, alter the interaction with other elements or induce an inflammatory or autoimmune response [47,48].

Human plasma is constituted of many proteins such as albumin (HSA) and fibrinogen, two of the most representative plasma proteins that are attached to the surface of several nanoparticles after entering the blood circulation [49]. For this reason, it is essential to analyses the effect of the dendrimers on those proteins, to ensure there will be no deleterious or unexpected effects upon interaction.

The haemolysis properties and interaction of the CS/PAMAM dendrimer NPs with plasma proteins are represented in Fig. 7(a) and (b), respectively.

The analysis of the CS/PAMAM dendrimer NPs showed the absence of haemolysis at any of the concentrations tested (Fig. 7(a)). The absorbance in the supernatant of the samples was similar to the absorbance of the negative control (only PBS). Hence, the CS/PAMAM dendrimer NPs are biocompatible with red blood cells.

Then it was evaluated the NPs interactions with plasma protein (Fig. 7(b) and (c)).

The comparison of the protein spectra, after incubation with the NPs, with the spectra of the proteins alone showed the absence of relevant spectral shifts, even at the highest concentration tested, namely 20 μL of the sample. Only a minor change was observed for HSA, probably associated with an interaction between the NPs and the protein. Hence, the NPs are safe regarding protein structure, although alterations in other plasma proteins cannot be ruled out from this experiment. However, the lack of cytotoxicity, haemolytic effect, or major protein structural changes showed the excellent hemocompatibility of the NPs and their suitability for an *in vivo* administration.

### *7.4. Assessment of metabolic activity, cell proliferation and TNF α capture by anti-TNF α Abs-CS/PAMAM dendrimer NPs in THP-1 cell line*

The influence of anti-TNF α Abs conjugation to PAMAM dendrimer NPs on metabolic activity and cell proliferation was evaluated using the THP-1 cell line. The previous experiments were performed with CS/PAMAM dendrimer NPs without anti-TNF α and the results did not show significant toxicity, in the different concentrations tested. In this assay, the THP-1 cells were incubated for 7 days with the anti-TNF α Abs-CS/

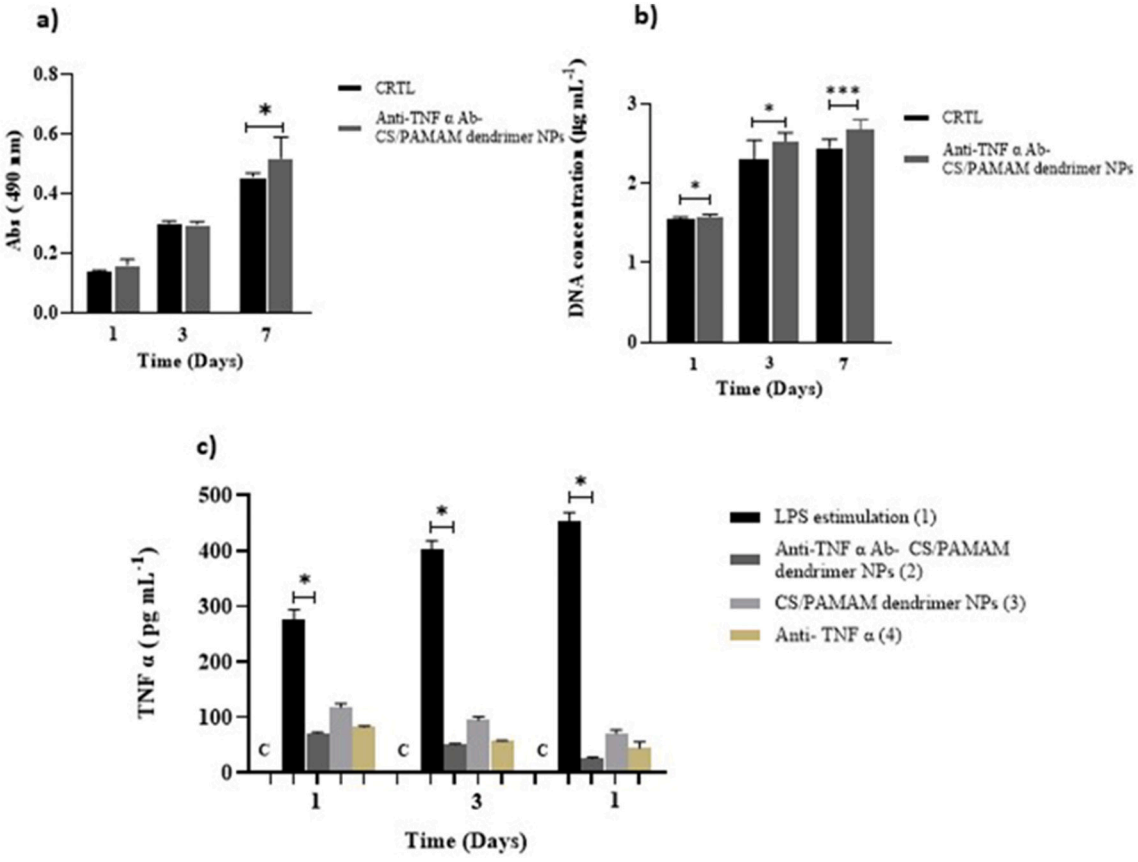


**Fig. 8.** Metabolic activity (a), Cell proliferation (b) and amount of uncaptured TNF α (c) under different conditions: cells differentiated with PMA but without LPS stimulation (C); cells stimulated with LPS,without treatment (1), anti-TNF α Abs-CS/PAMAM (2), CS/PAMAM, without Abs conjugated (3) and anti-TNF α Abs, (4) and. Significant differences *** $p < 0.001$ and *$p < 0.05$. Mann-Whitney test (a), Unpaired *t*-test (b) nonparametric Kruskal-Wallis test (c).

PAMAM dendrimer NPs (0.5 mg $mL^{-1}$), to assess the effect of this conjugation on cells' viability and proliferation.

The anti-TNF α Abs-CS/PAMAM dendrimer NPs' capacity to decrease the levels of TNF α present in the medium was evaluated using differentiated THP-1 cells, which were stimulated with LPS to induce an inflammatory scenario. Upon establishment of the inflammation, 4 conditions were tested: 1) cells without treatment, 2) cells with anti-TNF α Abs-CS/PAMAM dendrimer NPs, 3) cells with CS/PAMAM dendrimer NPs without Abs and 4) cells with anti-TNF α Abs alone. Cells differentiated with PMA but without LPS stimulation were used as control. Fig. 8 shows the metabolic activity and cell proliferation of THP-1 cells upon NPs administration and the quantity of free TNF α (uncaptured) over time of incubation with the NPs.

The cells' metabolic activity (Fig. 8a) and cell proliferation (Fig. 8b) were not affected by the presence of anti-TNF α Abs-CS/PAMAM dendrimer NPs when compared to control cells.

The TNF α capture by anti-TNF α Abs-CS/PAMAM dendrimer NPs and the capacity of the CS-modified dendrimer NPs to inhibit the release of TNF α were also evaluated. The results obtained showed that untreated LPS-stimulated cells presented high levels of free TNF α in the medium, compared to the remaining conditions, as expected. The levels of TNF α dropped significantly in the cells treated with anti-TNF α Abs CS/PAMAM dendrimer NPs, being even lower than the CS/PAMAM dendrimer NPs or the anti-TNF α Abs alone. Moreover, this trend was maintained throughout the time tested, as the TNF α levels continued decreasing up to 7 days (Fig. 8c).

The CS/PAMAM dendrimer NPs without anti-TNF α Abs also showed the ability to reduce TNF α levels significantly. These results are consistent with the literature that indicates that CS administration has an inhibitory effect on the release of TNF-α release, due to the anti-inflammatory activity of this sulphated glycosaminoglycan [50–52]. The combination of both effects, namely the anti-inflammatory effect of the CS and the presence of the anti-TNF α Abs, has probably increased the therapeutic efficacy of anti-TNF α Abs-CS/PAMAM dendrimer NPs by reducing the production and enhancing the capture of the pro-inflammatory cytokine. Although no statistically significant differences were observed, a trend was visible as the free TNF α decreases over time, with a more pronounced effect on the dendrimers with Abs, indicating a combined effect of the CS with the Abs.

Rheumatoid arthritis is characterised by an imbalance between a pro-inflammatory and anti-inflammatory cytokines, that is, upregulation of pro-inflammatory cytokines and downregulation of anti-inflammatory cytokines [53,54]. Since the pro-inflammatory phenotype is more evident in the synovial joints of patients with RA [55] only the pro-inflammatory cytokines were evaluated and more specifically TNF-α.

In fact, the model used in this study is a model of inflammation however, the inflammatory environment is a usual condition in rheumatoid arthritis. Through this model, it is possible to verify the anti-inflammatory effect of the anti-TNF α Abs-CS/PAMAM dendrimer NPs that can potentially be used in the treatment of several inflammatory pathologies including rheumatoid arthritis.

## 8. Conclusion

In this work, an innovative therapeutic approach comprising anti-TNF α Abs-CS/PAMAM dendrimer NPs was developed, to provide a more targeted and effective anti-inflammatory effect for the management of several inflammatory including RA disease. The main goal of this approach was to develop a therapeutic and efficient strategy,

through the maximum capture of TNF α by anti-TNF α Abs-CS/PAMAM dendrimer NPs and the synergistic inhibition of the inflammation by the CS. The proposed formulation showed appropriate mechanical and rheological properties and exhibited higher TNF α capture capacity than the anti-TNF α Abs alone, showing that this system could be useful for controlled and sustained drug delivery. The *in vitro* studies demonstrated that CS/PAMAM dendrimer NPs presence did not produce a deleterious effect on the tested cells' metabolic activity and proliferation, thus presenting a suitable cytocompatibility and hemocompatibility. The anti-TNF α Abs-CS/PAMAM dendrimer NPs properties owe them the potential to complement or improve current strategies in the treatment of rheumatoid arthritis.

## 9. Future perspective

Recent studies using dendrimers show their great specificity in the delivery of the drugs to the site of interest. Having this in mind, it was hypothesised that PAMAM dendrimer functionalised with CS and linked to specific antibodies (anti-TNF α) could help in the treatment of RA. The combinatory approach presented here showed a synergistic effect of capture ability of the target agent over time and reduction of this production, showing great potential to be used as a specific and sustained treatment in RA patients. Despite the encouraging results showed in this work, further studies are required to clarify the underlying mechanisms. Therefore, future work will comprise the proof of concept of this system *in vivo*, through an animal model of RA. In the future, dendrimers will undoubtedly have an important role in the world of nanopharmaceuticals, and in particular, in patient-specific approaches for RA treatment.

## CRediT authorship contribution statement

All of the authors (Isabel Maria Oliveira, Cristiana Gonçalves, Eduarda Pinheiro Oliveira, Rosana Simón-Vázquez, Alain da Silva Morais, África González-Fernández, Rui Luis Reis, and Joaquim Miguel Oliveira) declare that they have all participated in the design, execution, and analysis of the paper, and that they have approved the final version. Furthermore, each author certifies that this work is not under publication or consideration for publication in other journals.

## Declaration of competing interest

The authors declare that they have no known competing financial interests or personal relationships that could have appeared to influence the work reported in this paper.

## Acknowledgements

The authors thank the financial support under the Norte2020 project ("NORTE-08-5369-FSE-000044") and BD/137726/2018/J6 21340zkMF. The FCT distinction attributed to J. M. O. under the Investigator FCT program (number IF/01285/2015) is also greatly acknowledged. C. G. also wished to acknowledge FCT for supporting her research (No. SFRH/BPD/94277/2013). RS and AG-F thank Xunta de Galicia (Grupo de Referencia Competitiva, ED431C 2016041) and Centro de Investigaciones Biomédicas (CINBIO), Vigo, Spain, for supporting their research.

## References

[1] J.A. Singh, K.G. Saag, S.L. Bridges, E.A. Akl, R.R. Bannuru, M.C. Sullivan, E. Vaysbrot, C. McNaughton, M. Osani, R.H. Shmerling, Arthritis & rheumatology 68 (2016) 1–26.
[2] D.M. Gerlag, J.M. Norris, P.P. Tak, Rheumatology 55 (2016) 607–614.
[3] M. Yang, X. Feng, J. Ding, F. Chang, X. Chen, J. Control. Release 28 (2017) 108–124.
[4] G. Guidelli, T. Barskova, M. Brizi, G. Lepri, A. Parma, R. Talarico, L. Cantarini, B. Frediani, Clin. Exp. Rheumatol. 33 (2015) 102–108.
[5] H. Boulaiz, P.J. Alvarez, A. Ramirez, J.A. Marchal, J. Prados, F. Rodríguez-Serrano, M. Perán, C. Melguizo, A. Aranega, Int. J. Mol. Sci. 12 (2011) 3303–3321.
[6] I.M. Oliveira, C. Gonçalves, R.L. Reis, J.M. Oliveira, Nano Res. 11 (2018) 4489–4506.
[7] S. Kany, J.T. Vollrath, B. Relja, International journal of molecular sciences, 20 (2019) 6008.
[8] R. Neta, T. Sayers, J. Oppenheim, Immunol. Ser. 56 (1992) 499–566.
[9] H. Radner, D. Aletaha, Wien. Med. Wochenschr. 165 (2015) 3–9.
[10] D. Lombardo, M.A. Kiselev, M.T. Caccamo, Journal of Nanomaterials, 2019, 2019.
[11] J.K. Patra, G. Das, L.F. Fraceto, E.V.R. Campos, M. del Pilar Rodriguez-Torres, L.S. Acosta-Torres, L.A. Diaz-Torres, R. Grillo, M.K. Swamy, S. Sharma, Journal of Nanobiotechnology, 16 (2018) 71.
[12] B. Gorain, M. Tekade, P. Kesharwani, A.K. Iyer, K. Kalia, R.K. Tekade, Drug Discov. Today 22 (2017) 652–664.
[13] H. Wang, Q. Huang, H. Chang, J. Xiao, Y. Cheng, Biomaterials Science 4 (2016) 375–390.
[14] R. Qi, I. Majoros, A.C. Misra, A.E. Koch, P. Campbell, H. Marotte, I.L. Bergin, Z. Cao, S. Goonewardena, J. Morry, J. Biomed. Nanotechnol. 11 (2015) 1431–1441.
[15] D. Chandrasekar, R. Sistla, F.J. Ahmad, R.K. Khar, P.V. Diwan, J. Biomed. Mater. Res. A 82 (2007) 92–103.
[16] T.P. Thomas, S.N. Goonewardena, I.J. Majoros, A. Kotlyar, Z. Cao, P.R. Leroueil, J. R. Baker Jr., Arthritis & Rheumatism 63 (2011) 2671–2680.
[17] S. van Rijt, P. Habibovic, J. R. Soc. Interface 14 (2017) 20170093.
[18] S.R. Cerqueira, B.L. Silva, J.M. Oliveira, J.F. Mano, N. Sousa, A.J. Salgado, R.L. Reis, Macromol. Biosci. 12 (2012) 591–597.
[19] E.B. Bahadır, M.K. Sezgintürk, Talanta 148 (2016) 427–438.
[20] M. Nurunnabi, V. Revuri, K.M. Huh, Y.-k. Lee, Polysaccharide based nano/microformulation: an effective and versatile oral drug delivery system, Elsevier, Nanostructures for Oral Medicine, 2017, pp. 409–433.
[21] K. Nagasawa, H. Uchiyama, N. Wajima, Carbohydr. Res. 158 (1986) 183–190.
[22] M. Zaręba, P. Sareło, M. Kopaczyńska, A. Białońska, Ł. Uram, M. Walczak, D. Aebisher, S. Wołowiec, International Journal of Molecular Sciences, 20 (2019) 4998.
[23] V.K. Yellepeddi, A. Kumar, S. Palakurthi, Anticancer Res. 29 (2009) 2933–2943.
[24] J.S. Choi, K. Nam, J.-y. Park, J.-B. Kim, J.-K. Lee, J.-s. Park, J. Control. Release 99 (2004) 445–456.
[25] A. Khanlari, T.C. Suekama, S.H. Gehrke, Macromolecular Symposia, Wiley Online Library, 2015, pp. 67–77.
[26] V.H. Pomin, Anal. Chem. 86 (2014) 65–94.
[27] A.R. Fajardo, M.B. Silva, L.C. Lopes, J.F. Piai, A.F. Rubira, E.C. Muniz, RSC Adv. 2 (2012) 11095–11103.
[28] S. Lü, C. Gao, X. Xu, X. Bai, H. Duan, N. Gao, C. Feng, Y. Xiong, M. Liu, ACS Appl. Mater. Interfaces 7 (2015) 13029–13037.
[29] Y. Wang, P. Su, S. Wang, J. Wu, J. Huang, Y. Yang, J. Mater. Chem. B 1 (2013) 5028–5035.
[30] X. Zheng, T. Wang, H. Jiang, Y. Li, T. Jiang, J. Zhang, S. Wang, Asian Journal of Pharmaceutical Sciences, 8 (2013) 278–286.
[31] Y. Duan, Z. Xing, J. Yang, Y. Wang, J. Chen, Y. Zhang, W. Shi, Q. Li, RSC Adv. 6 (2016) 70870–70876.
[32] M.R. Carvalho, F.R. Maia, J. Silva-Correia, B.M. Costa, R.L. Reis, J.M. Oliveira, Nanomedicine 12 (2017) 581–596.
[33] M. Imamura, Y. Kodama, N. Higuchi, K. Kanda, H. Nakagawa, T. Muro, T. Nakamura, T. Kitahara, H. Sasaki, Biol. Pharm. Bull. 37 (2014) 552–559.
[34] F. Cilurzo, F. Selmin, P. Minghetti, M. Adami, E. Bertoni, S. Lauria, L. Montanari, AAPS PharmSciTech 12 (2011) 604–609.
[35] B. Wei, L. Romero-Zerón, D. Rodrigue, Journal of Macromolecular Science, Part B 53 (2014) 625–644.
[36] H. Yaich, H. Garna, S. Besbes, J.-P. Barthélemy, M. Paquot, C. Blecker, H. Attia, Food Hydrocoll. 40 (2014) 53–63.
[37] W. Wang, K. Gaus, R.D. Tilley, J.J. Gooding, Materials Horizons 6 (2019) 1538–1547.
[38] H.H. Gustafson, D. Holt-Casper, D.W. Grainger, H. Ghandehari, Nano Today 10 (2015) 487–510.
[39] Y.-W. Huang, M. Cambre, H.-J. Lee, International Journal of Molecular Sciences, 18 (2017) 2702.
[40] A. Janaszewska, J. Lazniewska, P. Trzepiński, M. Marcinkowska, B. Klajnert-Maculewicz, Biomolecules 9 (2019) 330.
[41] R. Simon-Vazquez, T. Lozano-Fernandez, A. Davila-Grana, A. Gonzalez-Fernandez, International Journal of Nanomedicine, 11 (2016) 4657.
[42] W. Chanput, J.J. Mes, H.J. Wichers, Int. Immunopharmacol. 23 (2014) 37–45.
[43] G. Arango Duque, A., Descoteaux, Front. Immunol. 5 (2014) 491.
[44] M.A. Dobrovolskaia, J.D. Clogston, B.W. Neun, J.B. Hall, A.K. Patri, S.E. McNeil, Nano Lett. 8 (2008) 2180–2187.
[45] J.-P. Boutrand, Biocompatibility and Performance of Medical Devices, Woodhead Publishing, 2019.
[46] S. Henkelman, G. Rakhorst, J. Blanton, W. van Oeveren, Mater. Sci. Eng. C 29 (2009) 1650–1654.
[47] R. Simón-Vázquez, T. Lozano-Fernández, M. Peleteiro-Olmedo, Á. González-Fernández, Colloids Surf. B: Biointerfaces 113 (2014) 198–206.
[48] P. Canoa, R. Simón-Vázquez, J. Popplewell, Á. González-Fernández, Biosens. Bioelectron. 74 (2015) 376–383.
[49] B.-J.L. Van Hong Nguyen, International Journal of Nanomedicine, 12 (2017) 3137.
[50] F. Ronca, L. Palmieri, P. Panicucci, G. Ronca, Osteoarthr. Cartil. 6 (1998) 14–21.

[51] S.E. Tully, M. Rawat, L.C. Hsieh-Wilson, J. Am. Chem. Soc. 128 (2006) 7740–7741.
[52] G.M. Campo, A. Avenoso, S. Campo, A.M. Ferlazzo, D. Altavilla, A. Calatroni, Arthritis Res Ther 5 (2003) R122.
[53] S. Mateen, A. Zafar, S. Moin, A.Q. Khan, S. Zubair, Clinica Chimica Acta; International Journal of Clinical Chemistry, 455 (2016) 161–171.
[54] B. Soler Palacios, L. Estrada-Capetillo, E. Izquierdo, G. Criado, C. Nieto, C. Municio, I. González-Alvaro, P. Sánchez-Mateos, J.L. Pablos, A.L. Corbí, A. Puig-Kröger, J. Pathol. 235 (2015) 515–526.
[55] X. Yang, Y. Chang, W. Wei, Cell Prolif. 53 (2020), e12854.